Original Research

Invited

On the Heating of Linear Conductive Structures as Guide Wires and Catheters in Interventional MRI

Wolfgang R. Nitz, PhD,[1,2]* Arnulf Oppelt, PhD,[2] Wolfgang Renz, PhD,[2] Christoph Manke, MD,[1] Markus Lenhart, MD,[1] and Johann Link, MD[1]

The interest in performing vascular interventions under magnetic resonance (MR) guidance has initiated the evaluation of the potential hazard of long conductive wires and catheters. The objective of this work is to present a simple analytical approach to address this concern and to demonstrate the agreement with experimental results. The first hypothesis is that a long conductive structure couples with the electric field of the radio frequency (RF) transmit coil. The second hypothesis is that this coupling induces high voltages near the wire ends. These voltages can cause tissue heating due to induced currents. The experimental results show an increase in coupling when moving a guide wire toward the wall of an RF transmit coil, documented with a temperature increase of a saline solution in close proximity to the tip of the guide wire. The coupling of the wire not only presents a potential hazard to the patient, but also interferes with the visualization of the wire. A safe alternative would be the use of nonconducting guide wires. J. Magn. Reson. Imaging 2001;13: 105–114. © 2001 Wiley-Liss, Inc.

Index terms: MRI-guided intervention; vascular interventions; interventional MRI; RF transmit coil; nonconducting guide wires

ENDOVASCULAR INTERVENTION using magnetic resonance imaging (MRI) is an area of increasing interest within the medical community. The high tissue contrast of magnetic resonance (MR), the convenient multiplanar imaging capability, the lack of ionizing radiation, and the low complication rate of MR contrast agents make this modality a promising alternative to conventional angiography in the future. However, there are still unresolved issues with respect to safety and reliable visualization of devices used in intravascular interventions. Most of the publications (1–4) dealing with novel MR techniques for visualization of guide wires and catheters point to the fact that a long conductive structure may operate as an antenna which causes an increase in power deposition around the wire or catheter. Unfortunately, this increased local specific absorption rate (SAR) is potentially harmful to the patient. Previously published safety relevant evaluations addressed the potential heating of intravascular coils (5). It has been demonstrated and documented that the heating is not related to transitions in the gradient fields, but due exclusively to coupling with the transmit radio frequency (RF) field. Further evaluations revealed three important points (6). First, the primary heating mechanism is via coupling to the long cable between the intravascular coil and the scanner. Second, placing the cable near the isocenter produces less heating. Third, heating is always detected near the tip of the coil, with no significant heating detected along the cable. In evaluating the visibility of commercial guide wires, catheters, and stents, it has been noted that the reported effects observed for a cable connecting an intravascular coil to a scanner interface are also to be observed for a conductive guide wire with no connection to the scanner (7).

In this article, an explanation is proposed for how a linear conductive structure couples with the *E*-field generated by the MR transmitter coil, and how this field can cause tissue heating primarily at the wire ends. The theory is validated with experiments using a simple straight conductive guide wire with no connection to the scanner and no connection to an intravascular coil. The experiments were designed to demonstrate the following:

1. The generated heat is confined in close proximity to the tip of the wire.
2. The heat generated in close proximity to the tip of a conductive guide wire is due to an interaction with the RF field, produced during transmission.
3. The heat generation in close proximity to the tip of a conductive guide wire is due to an interaction with the electric component of the RF field.
4. The length of the guide wire has an influence on the induced voltage and hence the induced current from the tip of the wire into the tissue.
5. The induced current on the wire generates B_1-field variations around the wire that also give rise to local signal variations.

[1]Department of Radiology, University of Regensburg, Germany.
[2]Siemens AG, Medical Engineering, MR Development, Erlangen, Germany.
*Address reprint requests to: W.R.N., Department of Diagnostic Radiology, University Hospital of Regensburg, D-93042 Regensburg, Germany. E-mail: wolfgang.nitz@klinik.uni-regensburg.de
Received March 3, 2000; Accepted July 31, 2000.

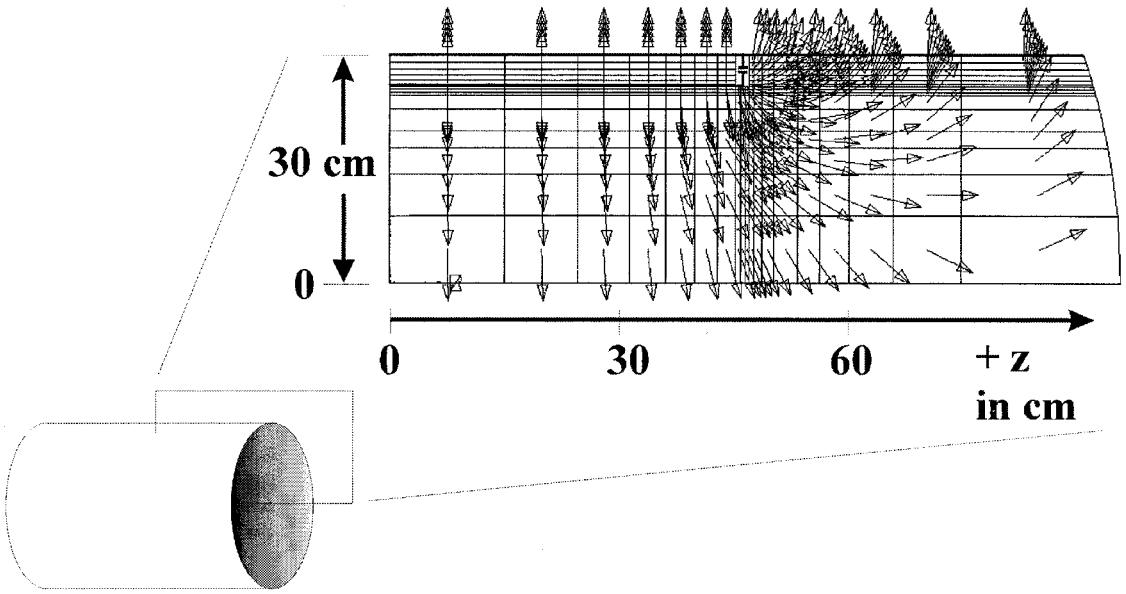

Figure 1. Example of the electric field distribution in an idealized RF resonator with a ring of capacitors at its ends. Shown is the upper right quadrant of the resonator.

THEORY

It is widely recognized that rapidly changing magnetic fields are generated either by the switching of gradient coils in MRI, or due to the applied RF fields. These fields can induce eddy currents in closed conducting loops that lead to heating. However, the behavior of linear conducting structures in MR scanners has only recently been the focus of scientific investigations. High temperature increases have been observed at the ends of metallic catheters and guide wires during evaluation of the safety of MR-guided vascular interventions (5–7). Since interventional angiography may become an important new application of MR in the future, a closer look at the physical principles of this effect is presented and an attempt is made to analyze the dependence on geometric parameters.

In addition to the magnetic component of the RF field necessary to generate transverse nuclear magnetization, an electric component of the RF field also exists in an MR scanner. This follows from Faraday's law, which requires that each alternating magnetic field is surrounded by an electric field according to

$$rot\ \vec{E} = -\frac{\partial}{\partial t}\vec{B} \qquad (1)$$

Therefore, the homogeneous RF magnetic field B_1 necessary in MR gives rise to a concentric electric field

$$\vec{E}(\vec{r}) = \frac{i}{2}\,\omega\vec{r} \times \vec{B} \qquad (2)$$

$$i = \sqrt{-1}$$

ω: angular frequency of the RF magnetic field B_1

r: radius

However, since the B_1 field cannot extend to infinity, an additional electric field component stemming from the conductors of the RF transmit coil is created and superimposed on the induced field at its borders. Its magnitude depends on the construction of the coil and is, in general, much larger than the inductive term mentioned above (Fig. 1).

A long conductor such as a wire in the electric field, E, of the RF transmit coil therefore has a voltage induced along its length

$$U_0 = \int_{l_1}^{l_2} \vec{E}d\vec{s} \qquad (3)$$

that drives an electric current through the wire. This current continues at the ends of the wire as an electric and a dielectric displacement current, causing heating in conductive tissue.

Next, consider the linear conductor as a transmission line consisting of two parts with lengths l_1 and l_2, being fed with U_0 at distance l_1 from one end (Fig. 2). The first part of the transmission line may be immersed into tissue characterized by permittivity ε_1 and conductivity σ_1, while the second part extends outside the magnet into air. This model represents a guidewire being inserted into a patient at the opening of a closed bore magnet.

The two parts of the transmission line are characterized by a distributed complex impedance

$$X'_{1,2} = R'_{1,2} + i\omega L'_{1,2} \qquad (4)$$

R': resistance per unit length

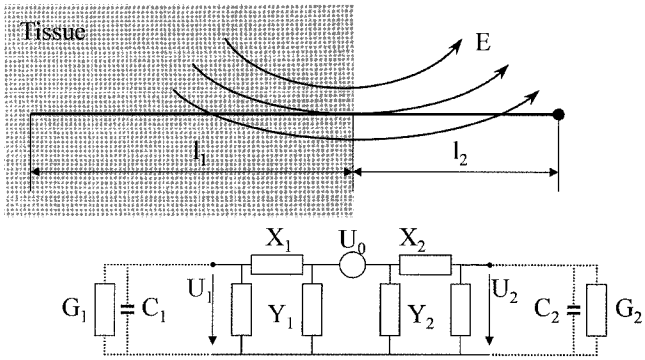

Figure 2. A linear conductor in an electric field E and its equivalent electric circuit.

$$L' = \frac{\mu}{2\pi} \ln \frac{2h}{r}\text{: inductance per unit length}$$

h: distance to ground

r: diameter of the wire

μ: susceptibility

and a distributed complex parallel conductance

$$Y'_{1,2} = G'_{1,2} + i\omega C'_{1,2} \tag{5}$$

$$C' = \frac{2\pi\varepsilon}{\ln \frac{2h}{r}}\text{: capacitance per unit length}$$

$$G' = \frac{2\pi\sigma}{\ln \frac{2h}{r}} = \frac{\sigma}{\varepsilon} C'\text{: conductance per unit length}$$

ε: permittivity

σ: conductivity

with

$$\gamma_{1,2} = \sqrt{(R'_{1,2} + i\omega L'_{1,2})(G'_{1,2} + i\omega C'_{1,2})} \tag{6}$$

as propagation constants and

$$Z'_{1,2} = \sqrt{\frac{R'_{1,2} + i\omega L'_{1,2}}{G'_{1,2} + i\omega C'_{1,2}}} \tag{7}$$

as wave impedances.

The electromagnetic waves travelling along the wire superimpose themselves at the wire ends, giving rise to a strong electric field. To analyze the effect of tissue heating, we will focus only on the effect of this field and neglect other field components along the wire. It is known from electric circuit theory that a wave guide can be characterized with respect to its ends by an equivalent four-pole circuit either in a T or a Π arrangement (8). Choosing a Π arrangement, we characterize the assumed two parts of the waveguide by the longitudinal impedances

$$X_{1,2} = Z_{1,2} \sinh \gamma_{1,2} l_{1,2} \tag{8a}$$

and the transversal conductances

$$Y_{1,2} = \frac{\tanh \frac{1}{2} \gamma_{1,2} l_{1,2}}{Z_{1,2}} \tag{9a}$$

For short lines, when $\gamma l \ll 1$ one can assume

$$X_{1,2} \approx (R_{1,2} + i\omega L_{1,2}) l_{1,2} \tag{8b}$$

and

$$Y_{1,2} \approx \frac{1}{2} (G_{1,2} + i\omega C_{1,2}) l_{1,2} \tag{9b}$$

Considering the endings of the conductor as spheres with radius $r_{1,2}$ representing a capacitance

$$C_{1,2} = 4\pi\varepsilon_{1,2} r_{1,2} \tag{10}$$

$\varepsilon_{1,2}$: permittivitivity of the surrounding, e.g., tissue

and a conductance

$$G_{1,2} = 4\pi\sigma_{1,2} r_{1,2} = \frac{\sigma}{\varepsilon} C_{1,2} \tag{11}$$

$\sigma_{1,2}$:

electric conductivity of the surrounding, i.e., tissue

the voltages $U_{1,2}$ at the wire ends gives rise to an electric field

$$E_{1,2} = U_{1,2} \frac{r_{1,2}}{r^2} \tag{12}$$

If the conductor is immersed in conductive tissue, the electric field at the wire ends drives a current density causing a loss of power density

$$P_{V_{1,2}}(r) = \frac{1}{2} \sigma_{1,2} E^2_{1,2} = \frac{\sigma_{1,2} U^2_{1,2} r^2_{1,2}}{2r^4} \tag{13a}$$

The temperature as measured with a small sensor directly at the conductor surface is determined by

$$P_{V_{1,2}}(r_0) = \frac{\sigma_{1,2} U^2_{1,2}}{2r^2_{1,2}} \tag{13b}$$

i.e., a sharp edge at the end of the conductor gets hotter than a smooth one.

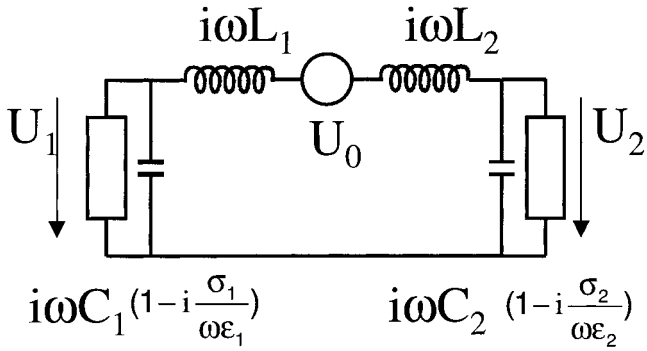

Figure 3. Simplified equivalent circuit of a guide wire in an MR scanner with part of the wire being inserted into tissue.

Power density at the conductor ends depends on wire radius, and also strongly on the voltage $U_{1,2}$ at the end. These voltages can be calculated from the equivalent circuit in Figure 2. To make things simple, the distributed capacitance is neglected. Hence

$$C'_{1,2}l_{1,2} \ll C_{1,2} \tag{14}$$

which is valid for a large distance between the wire and the system ground. We also consider the serial resistance of the wire to be negligible

$$R'_{1,2} \ll \omega L'_{1,2} \tag{15a}$$

This means that the wire pieces are characterized with respect to their ends by simple lumped inductances

$$L_{1,2} = L'_{1,2}l_{1,2} \tag{15b}$$

leading to the equivalent circuit of Figure 3. From this circuit, one obtains

$$U_{1,2} = \frac{U_0 C_{2,1}\left(1 - i\,\frac{\sigma_{2,1}}{\omega\varepsilon_{2,1}}\right)}{\left[1 - \frac{\omega^2}{\omega_1^2}\left(1 - i\,\frac{\sigma_1}{\omega\varepsilon_1}\right)\right]C_2\left(1 - i\,\frac{\sigma_2}{\omega\varepsilon_2}\right) + \left[1 - \frac{\omega^2}{\omega_2^2}\left(1 - i\,\frac{\sigma_2}{\omega\varepsilon_2}\right)\right]C_1\left(1 - i\,\frac{\sigma_1}{\omega\varepsilon_1}\right)} \tag{16a}$$

Assuming an equal radius for the guide wire ends ($r_1 = r_2$), the voltages at the wire ends are related by

$$\left|\frac{U_1}{U_2}\right| = \sqrt{\frac{\sigma_2^2 + \omega^2\varepsilon_2^2}{\sigma_1^2 + \omega^2\varepsilon_1^2}} \tag{16b}$$

so a surrounding medium with low conductivity at one wire end leads to a low voltage at the other. A guidewire introduced into a patient can achieve greatest temperature increase at the end in free air.

The voltages at the wire ends become a maximum at resonance frequencies

$$\omega_{1,2}^2 = \frac{1}{L_{1,2}C_{1,2}} \tag{17}$$

These resonant frequencies are determined by the geometric properties, l_1, l_2, of the transmission line describing the feeding point of the driving voltage U_0, and the electric properties $\varepsilon_{1,2}$, $\sigma_{1,2}$ of the medium surrounding the line. Since U_0 is not fed in at a sharp position but distributed over the total wire length, l_1 and l_2 have to be considered as averages in order to be able to model the wire.

Depending on the feeding point and the amount of length immersed in tissue, resonance can occur at different total wire lengths. Only for a center-fed wire completely immersed in tissue (or outside of it) with $l_1 = l_2$ would one observe a resonance at $l = \lambda/2$, i.e., the wire representing a $\lambda/2$ dipole antenna. Since the wire capacitance depends on the permittivity of the surrounding wire, the wavelength λ in tissue differs from the wavelength λ_0 in free air by

$$\lambda = \frac{\lambda_0}{\sqrt{\varepsilon_r}} \tag{18}$$

ε_r = relative permittivity

With a frequency of the applied RF pulse of 63585440 Hz on a 1.5T system, and the phase velocity in air $c_a = 2.9979 \cdot 10^8$ m/sec, the critical $\lambda/2$ wavelength in free air is 236 cm. For a conducting wire immersed in a dielectric poorly conducting medium like blood, the relative permittivity and relative permeability have to be considered, since both influence the phase velocity of the electromagnetic field

$$c = \frac{c_a}{\sqrt{\varepsilon_r\mu_r}} \tag{19}$$

The relative permeability takes into account the magnetic susceptibility—the ability to become magnetized. For water, the relative permeability is $\mu_r = 0.999991$. The relative permittivity takes into account the molecular polarizability. The value for water is 81 for a static electric field. The relative permittivity and the conductivity are frequency dependent. The increase in conductivity with frequency is associated with a decrease in permittivity. The relative permittivity for blood at 63 MHz is about 67 (9–11). The phase velocity within blood is therefore close to 3.66 10^7 m/sec and the critical $\lambda/2$ wavelength for a conductive guide wire immersed in blood becomes 28.8 cm.

From the above model one would conclude

- A linear conductor in an MR transmit coil will pick up a voltage which increases when moving the conductor towards the resonator walls.
- The induced voltage is transformed by the wave guide properties of the conductor into different voltages at the ends of the wire.
- Tissue at each end of the wire is heated. The smaller the radius of the wire, the higher the temperature increase.

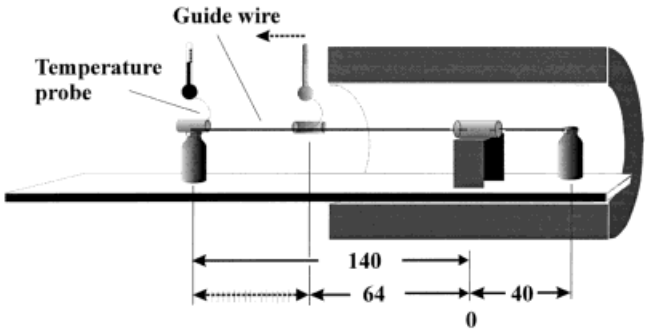

Figure 4. Experimental setup (experiment 1) for mapping a temperature increase toward the tip of the guide wire. The syringe with the temperature probe inside was slid 76 cm in 2-cm steps from the tip of the wire toward the isocenter of the magnet (+140 cm to +64 cm). After each move, an imaging sequence was executed and a temperature value was recorded.

- Wire resonance depends on wire length, permittivity and conductivity of the surroundings, and on the longitudinal wire position within the electric component of the RF field.

MATERIALS AND METHODS

Experiments were performed on a 1.5T whole-body imager (MAGNETOM Symphony, Siemens AG (Med), Erlangen, Germany). The circular polarized body resonator was used for transmitting as well as for receiving. A nonferromagnetic metallic guide wire was used to evaluate and demonstrate the coupling of a long linear conductive structure with the RF transmit field. The wire had a 0.89-mm diameter. It was constructed from a Nickel-Titanium tapered core with a polyurethane coating (radifocus guidewire, Terumo Corporation, Tokyo, Japan) and is commonly used to perform conventional interventional endovascular procedures under X-ray fluoroscopic guidance. Commercial wire lengths are 260 cm, 180 cm, and 150 cm. Temperatures were measured with an MR-compatible optical fiber temperature system (Model 750-Fluoroptic™ Thermometry System, Luxtron Corporation, Mountain View, CA) with as many as four probes. The temperature probes consisted of manganese-activated magnesium fluorogermanate; its fluorescent decay time is a function of temperature. The phosphor to fluoresce stimulation is provided by a xenon flash lamp. Twenty samples were collected simultaneously from all activated channels, with an interval of 0.1 sec/sample. This provided a precision of 0.22°C for all experiments. Temperature values were recorded manually by reading the digital display.

For the first experiment, a 180-cm-long wire was suspended in free air within the magnet, as shown in Figure 4. The wire was guided through a 1-L phantom filled with saline solution (plastic cylinder with a 8.6-cm diameter and 21-cm length) in order to simulate the influence of tissue, to image the B_1 field distribution around the wire, and to have a load for the transmitter coil. A 20-mL saline-filled syringe was placed at one end of the wire, and at the same location a Luxtron temperature sensor was mounted adjacent to the tip of the guide wire with silicone rubber. The tip of the wire and the tip of the sensor were outside of the silicone rubber tubing in order to measure the temperature increase of the adjacent saline solution. The wire extended in the $+z$ direction outside the magnet as one would expect for MR-guided endovascular interventional procedures. The position within the x-y plane was fixed at $x = +2$ cm and $y = +16$ cm. A fast low angle shot (FLASH) type sequence was used with the following scan parameters: 195 Hz/pixel, gradient motion rephasing (GMR), 14-msec repetition time (TR), 6.1-msec echo time (TE), 10-mm slice thickness, 256 * 256 matrix, 186-mm field of view (FOV), body coil excitation, and 16 acquisitions. This leads to a measurement time of 58 sec and a whole-body SAR of 1.28 W/kg. This protocol is sufficient to simulate worst case situations from near-real-time imaging to Turbo Spin Echo (TSE) applications. The 20-mL saline-filled syringe with the silicone rubber mounted fluoro-optic thermometer inside was positioned along the length of the wire from its tip toward the center of the magnet. It was slid along the wire in discrete 2-cm steps. The imaging protocol and act of recording the measured temperature changes at the end of each measurement were repeated at each location. The measurement was repeated using a true fast imaging with steady precession (trueFISP) protocol with the parameter: 260 Hz/pixel, 5.98-msec TR, 3-msec TE, 8-mm slice thickness, 256 * 256 matrix, 240-mm FOV, body coil, 8 acquisitions leading to a measurement time of 12 seconds, and a whole-body SAR of 1.11 W/kg. This sequence is also suitable for fast, real-time, and interactive imaging.

A second experiment was designed to measure the temperature change at the tip of the wire as a function of the excitation angle to confirm the dependency on the RF field. According to the theory, heat is generated by the induced voltages at the wire ends and the associated dissipation from currents is driven through the saline solution. A 180-cm guidewire was mounted on a water-filled plastic container. The guidewire was placed through 10-mL saline-filled syringes at position +130 cm (position 1), +46 cm (position 2), and −50 cm (position 3) relative to the isocenter of the magnet (Fig. 5). The x- and y-positions of the previous experiment were maintained. At position 1 and 2, the Luxtron tempera-

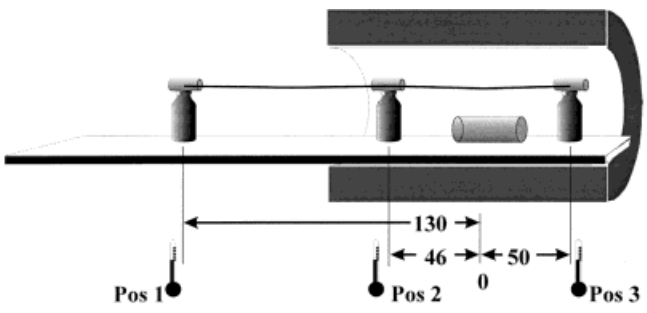

Figure 5. Experimental setup (experiment 2) for mapping a temperature as a function of the RF excitation angle. Temperature values were recorded at the three illustrated locations (Pos 1, Pos 2, and Pos 3).

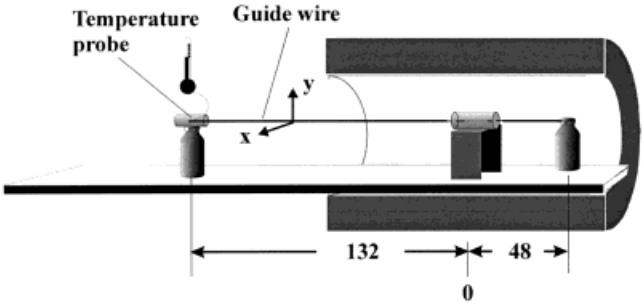

Figure 6. Experimental setup (experiment 3) for mapping a temperature increase at the tip of the guide wire as a function of *x*-*y* position. The guide wire always remained aligned parallel to the *z*-direction. The guide wire was moved together with syringes, phantoms, and supporting structures in *x*- and *y*-direction. For each location an imaging sequence was executed and temperature values were recorded at the end of each measurement.

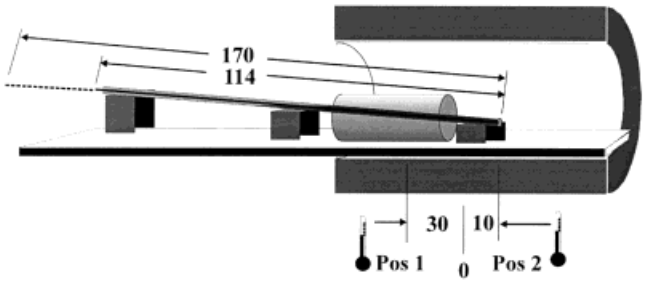

Figure 7. Experimental setup (experiment 4) for mapping a temperature increase in close proximity to the guide wire at two locations. The wire was partially immersed in a saline solution. One end of the wire at $z = -10$ cm was attached to a temperature probe (Pos 2). Another temperature probe was adjacent to the wire at position $z = +30$ cm (Pos 1). The guide wire was reduced in length in 2-cm steps from 170 cm to 114 cm. After each cut, an imaging sequence was executed and temperature values were taken at the end of each measurement.

ture probes were coupled with the guide wire using tight silicone tubes filled with a compound acting as a thermal conductor. At position 3, the temperature probe was adjacent to the wire end with no direct contact. The previously mentioned trueFISP protocol was applied using seven acquisitions for a 10-sec measurement time. The protocol was repeatedly executed, changing only the excitation angles from 5° to 100° in steps of 5° between measurements. Temperature values were recorded at the end of each measurement.

The third experiment was to confirm the increase in temperature change when moving the wire from the magnet isocenter towards the resonator wall in either the *x*- or *y*-direction. The previously mentioned FLASH protocol (1.28-W/kg SAR) was used. The guide wire was kept straight and parallel to the *z*-direction, and moved to all possible locations following discrete 4-cm steps in the *x*-direction and in 2-cm steps in the *y*-direction (Fig. 6). At each position, the imaging protocol was executed and the temperature in the vicinity of the tip of the guide wire was recorded at the end of each measurement.

A fourth experiment designed to detect any critical guide wire lengths was also performed. A 170-cm-long guide wire was placed in a 40-mL saline solution within an 8-mm diameter-rigid polyvinylchloride (PVC) tube (Fig. 7). This arrangement was to approximate the situation within a blood vessel. One temperature probe was mounted to the wire with a silicone tube at position $z = +30$ cm (position 1), another at position $z = -10$ cm (position 2) adjacent to the end of the guide wire. The wire was then cut at the distal end outside the magnet to reduce the total length from 170 cm to 114 cm in 2-cm steps. The imaging protocol was identical to the previous experiment.

A fifth experiment was designed to allow a determination of the relationship between temperature, B_1 alterations, and guide wire length. In these experiments, the imaging plane was perpendicular to the wire, at the isocenter of the magnet, documenting signal variations in the vicinity of the wire. A 180-cm-long guidewire was led through a 20-mL saline-filled syringe at position $z = +130$ cm (position 1); a temperature probe was attached at this location via tight silicone tubing. The wire was further guided through the 1-L saline-filled phantom and terminated in a 10-mL saline-filled syringe at position $z = -20$ cm (position 2). At that position, a temperature probe was mounted to the wire tip using a tight silicone tubing (Fig. 8). A FLASH type sequence was used not only for generating heat in the vicinity of the tip of the guidewire, but also for demonstrating the interference pattern between the B_1 field generated by the transmitting body resonator and the currents induced on the conductive guidewire by generating an image of an axial slice through the 1-L phantom. Sequence parameters were: 195 Hz/pixel, GMR, 14-ms TR, 6.1-ms TE, 6-mm slice thickness, 128 * 256 matrix, 186-mm FOV, 16 acquisitions leading to a measurement time of 30 sec and a 0.6-W/kg whole-body SAR). The wire was reduced in length from 180 cm to 156 cm in 2-cm steps. Cutting of the wire was done at the location outside of the magnet bore. After each cut the FLASH imaging sequence was executed and tem-

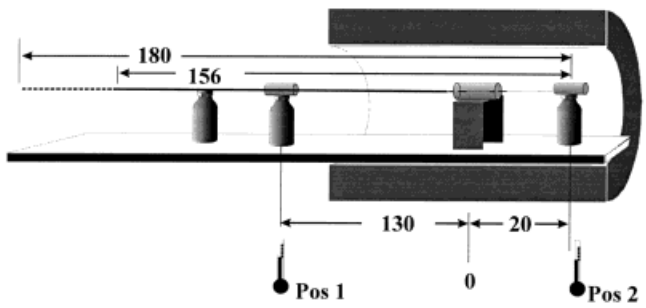

Figure 8. Experimental setup (experiment 5) for mapping a temperature increase in close proximity to the guide wire at two locations. The wire was suspended in free air with the exception of two 20-mL saline-filled syringes and a 1-L saline-filled phantom. The guide wire was reduced in length in 2-cm steps from 180 cm to 156 cm. After each cut, an imaging sequence was executed and temperature values were taken at the end of each measurement.

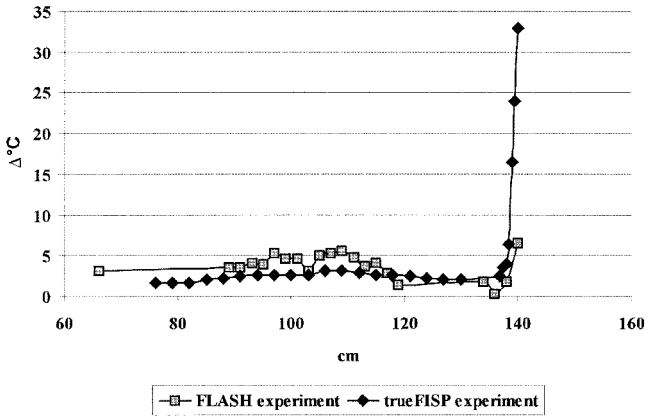

Figure 9. Temperature course along the wire (experiment 1). The 140-cm position marks the tip of the guide wire.

perature values were taken at the illustrated locations at the end of each measurement.

In a sixth experiment, we varied the asymmetry of the guide wire with respect to the 1-L saline-filled phantom positioned in the isocenter of the magnet, to demonstrate the sensitivity of the coupling with respect to an asymmetric placement in the *z*-direction.

RESULTS

According to the theory, a voltage builds up toward the wire ends, and this voltage will cause tissue heating due to dielectric and resistive losses. Figure 9 shows the measured temperature distribution as a function of the distance from the isocenter toward one wire end outside of the magnet, as determined with the temperature sensor close to the wire within a saline solution (Experiment 1). A 34°C temperature change was measured at the tip of the wire, dropping to a 24°C change 5 mm distal to the tip.

The temperature increase as a function of the excitation angle was recorded with the second experiment. The guide wire was guided through three syringes with saline solutions. The temperature increase was only

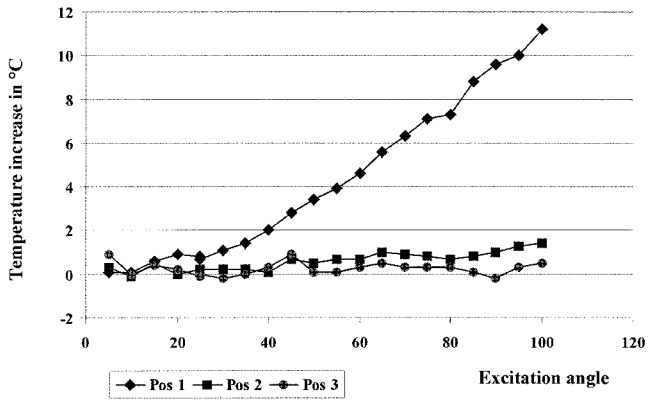

Figure 10. Results of experiment (experiment 2). Temperature adjacent to the guide wire in saline-filled syringes as a function of guide wire length.

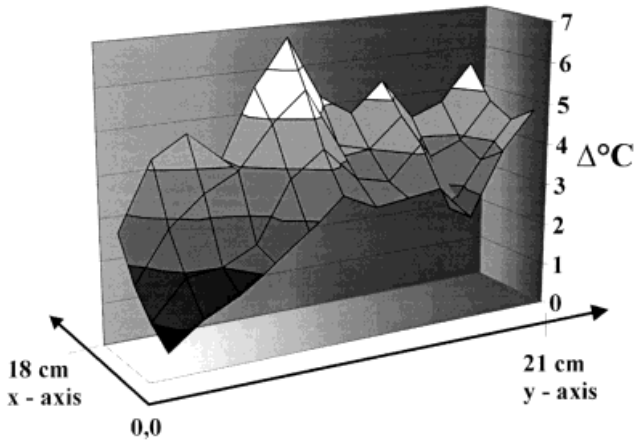

Figure 11. Temperature increase at the tip of the guide wire as a function of position within the resonator (experiment 3). A temperature rise of up to 6.7°C was measured at the 'soft' tip of the guide wire (thinning of the wire, polyurethane coating).

noticed at the end of the wire usually outside of the patient, whereas no significant temperature increase was recorded in the middle of the wire, or at the other end, usually located within the patient. The result of the temperature increase as a function of the excitation angle is given in Figure 10. A temperature change of less than 1°C was observed below an excitation angle of 30°.

There is a very strong correlation between the position of the wire in the *x*-*y* plane (with the wire aligned parallel to the *z*-direction) and the recorded temperature changes as found in the third experiment. The closer the wire is located toward the resonator wall, the further it is dislocated from the isocenter of the magnet, the larger the recorded temperature change at the tip of the wire after execution of the imaging protocol. This is in accordance with the hypothesis that it is the electric field within the MR transmit coil that couples with the wire. The temperature map as a function of the *x* and *y* position is given in Figure 11.

During the fourth experiment, the length of the guide wire was modified. The temperature changes as a func-

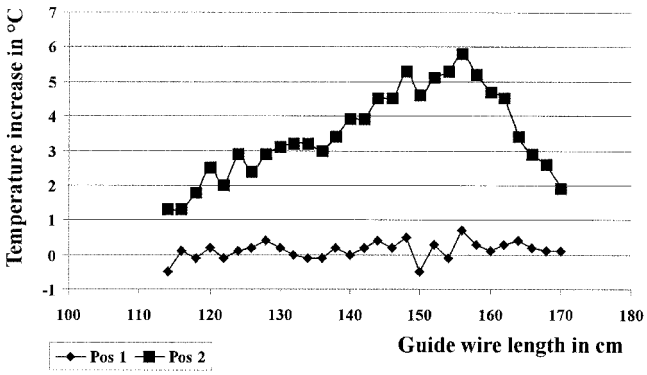

Figure 12. Results of experiment 4. Temperature increase as a function of guide wire length.

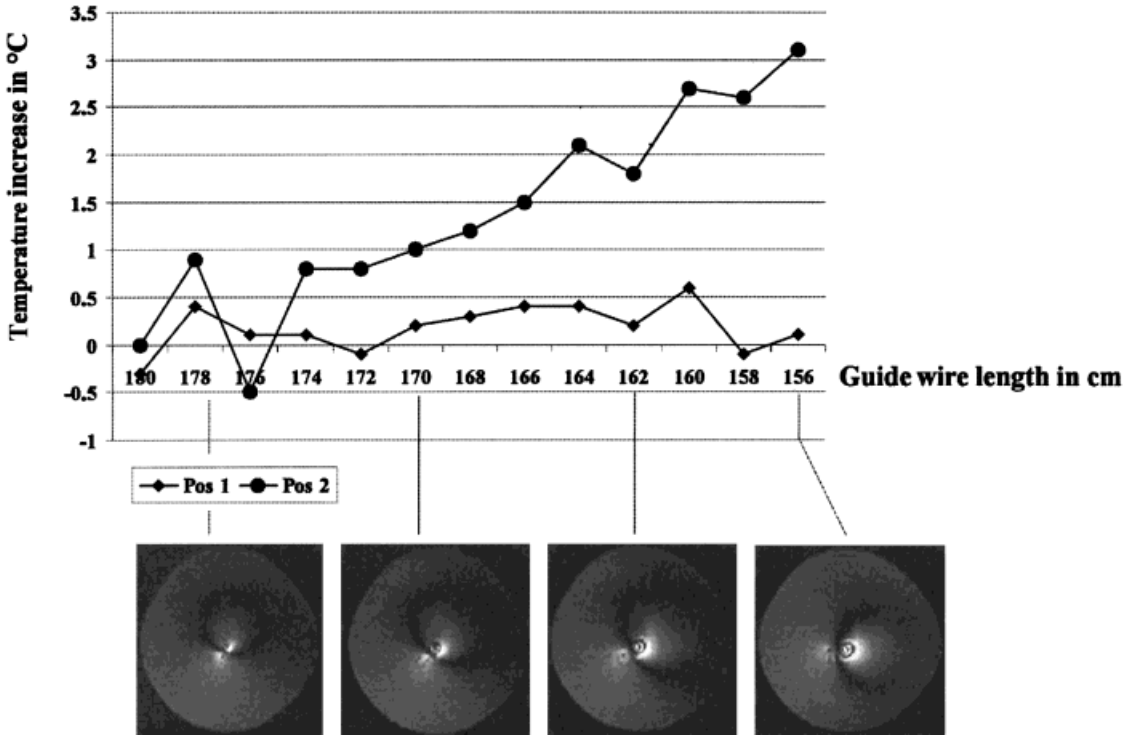

Figure 13. Results of experiment 5. Temperature increase as a function of guide wire length and transverse images documenting the change in B_1-field distribution.

tion of guide wire length are documented in Figure 12. In this experiment, a temperature increase was observed at the end of the wire usually inside the patient. The temperature change ranged from 2°C for a 170-cm guide wire length to a 6°C rise to for a 156-cm guide wire length. The temperature increase drops to 1°C for a 116-cm length. This demonstrates a very broad resonance, with the length of the wire as parameter.

The fifth experiment allowed simultaneous imaging of the B_1 field alterations and temperature recording. Again, a temperature increase was observed only at the location usually within the patient. We also observed signal variations almost symmetrically to the guide wire, for imaging sections perpendicular to the wire within the 1-L phantom filled with saline solution. We ascribe this effect to altered excitation angles due to the superposition of the RF magnetic field of the transmit coil and a magnetic field generated by the currents induced in the wire. Besides the B_1 field changes causing ring-shaped signal variations around the wire, the induced currents on the wire produce a sharply delineated ghost image of the wire itself. That ghost image is shifted in the x- and y-direction. The shift depends on the geometry of the phantom used, the length of the wire, the asymmetry with respect to the isocenter of the magnet and whether somebody is touching the wire or not. For the wire length with the largest recorded temperature change, sparking of the wire was observed when touching the wire during execution of an imaging protocol including a significant heat sensation and the ghost within the image, as well as the signal intensities around the location of the ghost and the original position of the wire, were also at a maximum. Figure 13 shows the recorded temperature change as a function of the guidewire length and gives four examples of the signal pattern of images acquired perpendicular to the wire.

It has been shown in earlier experiments (7) that the rotating ghost of the wire seems to be a much more sensitive indication of closeness to a resonance than a temperature measurement. The large changes in signal variations are always visible, whereas the heat generation at the tips of the conductive structure are sometimes missed, if the thermometer is not close enough to the tip of the wire or if the thermometer is attached to the wire with a poor thermal contact to the surrounding saline solution. We want to mention that not only a current is induced in the wire by the electric component of the RF transmit field causing variations of the B_1 field around the wire (and hence local signal variations due to varying flip angles), but also that the receiving profile is altered via the principle of reciprocity. Since the position of the ghost is not a function of repetition time or excitation angle, we believe that it represents a region around the wire where the RFs receive magnetic fields of the wire and coil cancel. Changing the resonance frequency of the wire can cause a phase shift between the electromagnetic (EM) fields of the wire and the receive coil, resulting in a rotation of the ghost when a circular polarized receive coil is used. We have observed that the temperature change at the tip of the wire reaches a maximum at the time the ghost appears only shifted in the x-direction. We also observed that a change of wire position in the phantom, as shown in Figure 14 (experiment 6), changes the RF-field distribution around the wire, then causes the ghost to be

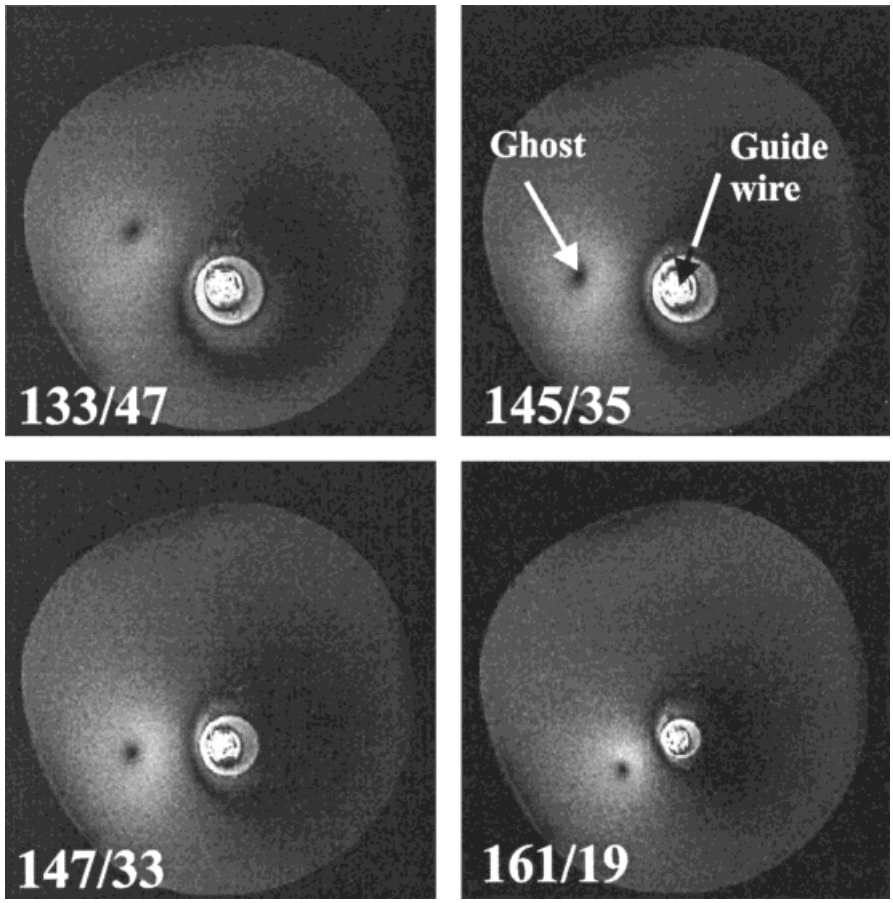

Figure 14. Rotating ghost (weak in intensity) of a guide wire and circular signal variations as a function of the wire asymmetry to the isocenter of the magnet (experiment 6); E.g., 133/47 is indicating an extension of the guide wire from 0 to +133 cm and from 0 to −47 cm in the *z*-direction.

shifted to a different position. A small shift in position has also been observed when moving the wire toward the resonator wall.

DISCUSSION

The potential hazard of a relatively long conductive structure has been referred to in all attempts to actively visualize catheters (1–5) in MR-guided vascular interventions, and in the evaluation of commercially available devices (12) currently used for conventional angiography under X-ray fluoroscopic guidance. It is not obvious that the safety-relevant issues discussed for EKG leads or connections to intravascular coils are also applicable to a simple conductive guide wire. Theory and experiments point to the same phenomenon of a coupling with the *E*-field component of the transmitted RF. The consequences are identical for both an isolated guide wire or a long connector to an intravascular coil. The interaction with the RF field is proven with the dependency on excitation angle. That it is the *E*-field component of the transmitted RF is concluded by the dependency on position relative to the RF resonator coil. The conductivity of currently used guide wire and the correlated potential heating in close proximity of the wire is seen as a major obstacle, preventing initial utilization of MR-guided vascular interventions. In all experiments where we imaged perpendicular to the wire guided through a signal emitting medium, we found the signal variation pattern to be expected for B_1 field alterations and a sharply delineated ghost. In repeated experiments with slightly altered configurations, we found a correlation between the position of this ghost and a traceable temperature change in the vicinity of the tip of the guide wire. We also observed maximal amplitudes for the signal alterations at the same time we documented maximal temperature changes. The appearance of the ghost and the intensity variations around the wire are a more sensitive indication for the coupling of the wire with the RF field than the temperature measurement in the vicinity of the tip of the guide wire. While repeating the experiment for (almost) the same experimental setup, we often failed to trace any temperature changes since those are confined to a very small region around the tip of the wire; we always were able to generate the images with the signal variation pattern indicating coupling of the wire with the RF field. Ghost and signal variations vanish when moving the guide wire to the center of the resonator, as do any traceable temperature changes.

Placement of a guide wire is basically the second step in an endovascular procedure, following puncture of the artery. A guide wire has to be inserted to serve as a path for interventional devices to follow. That guide wire has to be placed within the vessel lumen, should not cause a dissection of the wall during that procedure, has to pass the pathologic area, and is supposed to guide catheters with markers, a stent, or a balloon. The currently used state-of-the-art guide wires are made of a Nickel-Titanium alloy (nitinol) with a polyurethane

cover and provide unsurpassed mechanical properties. Since this is a non-ferromagnetic material, the B_0 inhomogeneity-related artifacts are visually small and confined to a submillimeter region around the material. Unfortunately, the wire is also a conductor which couples with the *E*-field of the RF pulse used in MR imaging. Commercially available plastic wires do not have the desirable mechanical properties of the nitinol material. Guide wires with a stainless steel core have an even better conductivity than the nitinol wire and are in addition sensitive to magnetic forces. The recent literature on active tracking also refer to the conductive guide wire as an open safety issue (13–16). Exceeding the measurements of Liu et al. (17) and Wildermuth et al. (5), we noted a temperature rise of up to 44°C within the saline solution adjacent to the guide wire tip in a measurement time of less than 12 sec with a trueFISP fast-imaging protocol. Konings et al. (18) reported a possible temperature increase of up to 72°C for an in vitro model of a stenotic vessel, attributing this effect to energy stored in resonating transverse electromagnetic waves. Our experimental results confirm our simple theory describing a conductive guide wire as a waveguide coupling with the *E*-field of the transmit resonator. The results indicate that the achieved temperature changes strongly depend on the position of the wire within the resonator and that the maximum temperature rise is to be expected at the tip of the wire. Besides the safety issue addressed in this work, it should be kept in mind that the coupling of the wire causes B_1-field variations that obscure the original wire position, hampering the necessary visualization and tracking of the guide wire. There seems to be no alternative than to seek out more sophisticated approaches with conductive material (14), or to use nonconductive guide wires.

REFERENCES

1. Dumoulin CL, Souza SP, Darrow RD. Real-time position monitoring of invasive devices using magnetic resonance. Magn Reson Med 1993;29:411–415.
2. Leung DA, Debatin JF, Wildermuth S, et al. Intravascular MR tracking catheter: preliminary experimental evaluation. AJR Am J Roentgenol 1995;164:1265–1270.
3. Atalar E, Kraitchman DL, Carkhuff B, et al. Catheter-tracking FOV MR fluoroscopy. Magn Reson Med 1998;40:865–872.
4. Glowinsky A, Adam G, Brücker A, Neuerburg J, van Vaals JJ, Günther RW. Catheter visualization using locally induced, actively controlled field inhomogeneities. Magn Reson Med 1997;38:253–258.
5. Wildermuth S, Dumoulin CL, Pfammatter T, Maier SE, Hofmann E, Debatin J. MR-guided percutaneous angioplasty: assessment of tracking safety, catheter handling and functionality. Cardiovasc Intervent Radiol 1998;21:404–410.
6. Ladd ME, Quick HH, Boesiger P, McKinnon GC. RF heating of actively visualized catheters and guidewires. In: Proceedings of the ISMRM, 6th Scientific Meeting and Exhibition, Sydney, 1998. p 473.
7. Nitz WR, Manke C, Lenhart M, Völk M, Fischer H, Oppelt A. Potential hazards using guidewires in MR guided vascular interventions (Abstr). Radiology 85th RSNA 1999;213(Suppl):367.
8. K. Küpfmüller. Einführung in die theoretische Elektrotechnik, 9. Auflage, 1969. Berlin/Heidelberg/New York: Springer Verlag.
9. Schwan PH. Electrical properties of blood and its constituents. Alternating current spectroscopy. Blut 1983;46:185–197.
10. Stoy RD, Foster KR, Schwan HP. Dielectric properties of mammalian tissues from 0.1 to 100 MHz: a summary of recent data. Phys Med Biol 1982;27:501–513.
11. Kraszewski A, Stuchly MA, Stuchly SS, Smith AM. In vivo and in vitro dielectric properties of animal tissues at radio frequencies. Bioelectromagnetics 1982;3:421–432.
12. Köchli VD, McKinnon GC, Hofmann E, von Schulthess GK. Vascular interventions guided by ultrafast MR imaging: evaluation of different materials. Magn Reson Med 1994;31:309–314.
13. Bakker CJ, Hoogeveen RM, Hurtak WF, van Vaals JJ, Viergever MA, Mali WPTM. MR-guided endovascular interventions: susceptibility-based catheter and near-real-time imaging technique. Radiology 1997;202:273–276.
14. Adam G, Glowinski A, Neuerburg J, Bücker A, van Vaals JJ, Günther RW. Visualization of MR-compatible catheters by electrically induced local field inhomogeneities: evaluation in vivo. J Magn Reson Imaging 1998;8:209–213.
15. Ladd ME, Erhart P, Debatin JF, et al. Guidewire antennas for MR fluoroscopy. Magn Reson Med 1997;37:891–897.
16. Kee TS, Rhee JS, Butts K, et al. MR-guided transjugular portosystemic shunt placement in a swine model. J Vasc Interv Radiol 1999;10:529–535.
17. Liu C-Y, Farahani K, Lu DSK, Duckwiler G, Oppelt A. Safety of MRI-guided endovascular guidewire applications. J Magn Reson Imaging 2000;12:75–78.
18. Konings MK, Bartels LW, Smits HFM, Bakker CJG. Heating around intravascular guidewires by resonating RF waves. J Magn Reson Imaging 2000;12:79–85.
19. Ladd ME, Quick HH. Reduction of resonant RF heating in intravascular catheters using coaxial chokes. Magn Reson Med 2000; 43:615–619.